



Assessment of aerodynamic behaviour and weight reduction

Deliverable 6.2

Author: Petr Vrchota
Date: 07/07/2020
Version: v1

Grant Agreement number: 723167
Project acronym: ACASIAS
Project title: Advanced Concepts for Aero-Structures
with Integrated Antennas and Sensors
Funding scheme: RIA
Start date of the project: 01/06/2017
Duration: 36 months
Project coordinator (organisation): Harmen Schippers (NLR)
Phone: 0031 (0)88-5114635
E-mail: Harmen.Schippers@nlr.nl
Project website address: www.acasias-project.eu





This project has received funding from the European Union's Horizon 2020 research and innovation programme under grant agreement No 723167

DOCUMENT INFORMATION

Document Name	Assessment of aerodynamic behaviour and weight reduction
Version	1
Version Date	07/07/2020
Author	Petr Vrchota
Security	CO

APPROVALS

	Name	Company	Date	Visa
Coordinator	H. Schippers	NLR	07/07/2020	
WP Leader	Z. Řezníček	EVEKTOR	07/07/2020	
Other (Quality M., AB)	A. Hoque	L-UP	06/07/2020	

DOCUMENTS HISTORY

Version	Date	Modification	Authors
0.1	22/10/2019	Initial draft version	P. Vrchota
0.2	20/03/2020	Results of Panasonic-like radome added	P. Vrchota
0.3	24/04/2020	Values of drag coefficient of particular configurations of CRM w/o radome were added	P. Vrchota
0.4	02/06/2020	Emissions of A-350 with Panasonic-like radome and Fokker 100 with Gogo-2Ku-like radome	P. Vrchota
V1	07/07/2020	Quality Review	A. Hoque

LIST OF AUTHORS

Full name	Organisation
Petr Vrchota	VZLU

DISTRIBUTION LIST

Full Name or Group	Organisation
All partners	ACASIAS
Miguel-Angel Marti-Vidal	EC

Contents

1. INTRODUCTION	5
2. MODELS.....	7
2.1. AIRCRAFT MODELS.....	7
2.2. ANTENNAS.....	8
3. METHODS.....	12
3.1. GRID GENERATION AND FLOW SOLVER	12
3.2. FLOW CONDITIONS	12
3.3. WEIGHT PENALTY	12
3.4. CARBON DIOXIDE (CO ₂) AND NITROGEN DIOXIDE (NO _x) EMISSIONS	13
4. RESULTS.....	15
4.1. EFFECT OF THE LOCATION OF THE RADOME ON THE DRAG	15
4.2. WEIGHT PENALTY	18
4.3. POSSIBLE REDUCTION OF THE CO ₂ AND NO _x EMISSIONS BY INTEGRATED ANTENNAS	21
5. CONCLUSIONS	26
6. REFERENCES	27

List of Abbreviations

ACASIAS	Advanced Concepts for Aero-Structures with Integrated Antennas and Sensors	GPS	Global Positioning System
AEDP	Aerodynamic Equivalent Drag Penalty	HC	Hydrocarbons
CAD	Computer Aided Design	H₂O	Dihydrogen Monoxide
CFD	Computational Fluid Dynamics	ICAO	International Civil Aviation Organisation
CL	Lift Coefficient	Ku	Kurz-unten
CO	Carbon Monoxide	L/D	Lift/Drag
CO₂	Carbon Dioxide	M	Mach
Cp	Pressure Coefficient	MTOW	Maximum Take-Off Mass
CRM	Common Research Model	NO_x	Nitrogen Dioxide
CROR	Contra-Rotating Open Rotor	NASA	National Aeronautics and Space Administration
DPW	Drag Prediction Workshops	OEW	Basic Operating Weight
EARSM	Explicit Algebraic Reynolds Stress Model	SATCOM	Satellite Communication
FML	Fibre Metal Laminate	VHF	Very High Frequency

1. Introduction

For communication and navigation purposes several protruding antennas and radomes are presently installed on board of aircraft. The installation of a Ku-band Satellite Communication (SATCOM) antenna requires the use of a radome on top of the fuselage. Many passenger aircraft are currently equipped with either a Panasonic antenna or a GoGo antenna. Their radomes are shown in Figure 1 and Figure 2, respectively. Classical Very High Frequency (VHF) communication antennas on aircraft behave aerodynamically as small wings. The installation of antennas and radomes will contribute to an increase of aerodynamic drag, and thus an increase of fuel consumption and Carbon Dioxide (CO₂) and NO_x emissions.



Figure 1: Radome for installation of Ku-band Panasonic antenna



Figure 2: Radome for installation of GoGo Ku-band antenna

The European ACASIAS project (Advanced Concepts for Aero-Structures with Integrated Antennas and Sensors) was launched in June 2017. The goal of ACASIAS is to reduce the fuel consumption of future aircraft by improving aerodynamic performance and by facilitating integration of new and efficient propulsion systems. ACASIAS will thus help to reduce CO₂ and NO_x emissions by aircraft and thus help to make aviation more sustainable.

ACASIAS is focused on developing innovative aircraft structures with additional functions. Research and development in ACASIAS are mainly focussed towards the structural integration of antennas used for communication purposes. In particular, the research is dedicated to developing:

1. a composite panel with an integrated Ku band antenna for satellite communication;
2. a winglet with an integrated VHF antenna;
3. a Fibre-Metal Laminate (FML) panel with an integrated VHF communication slot antenna and Global Positioning System (GPS) patch antenna;
4. a Sandwich lining panel for reduction of engine cabin noise with the aim to facilitate the installation of Contra-Rotating Open Rotor (CROR) engines.

The aim of the present report is to evaluate the effect of the conformal integration of communication VHF antennas and Ku-band satcom antennas with the surface of airplane to estimate the reduction of drag, fuel consumption and emissions by means of Computational Fluid Dynamics (CFD) simulations. The structurally integrated antennas are expected to cause less additional drag, noise and turbulence in comparison with classical protruding antennas. To this end the following airplanes have been considered:

- National Aeronautics and Space Administration (NASA) Common Research Model (CRM), representing a large twin-aisle aircraft such as A350 or Boeing787.
- Fokker 100 aircraft.
- Evktor EV-55 aircraft.

In order to estimate the increase of drag both the Panasonic-like radome (see Figure 1) and the GoGo-2Ku-like radome (see Figure 2) were placed on different positions on top of the fuselage of CRM. The Gogo-2Ku-like radome was only placed on the fuselage of the Fokker 100 aircraft. The VHF communication antennas were placed on the Fokker 100 aircraft and on the Evektor EV-55 aircraft.

The aerodynamic equivalent weight penalty and additional fuel needed due to the drag of radomes and antennas have been calculated.

The results of CFD simulations have also been used for the estimation of the CO₂ and NO_x emissions reduction.

2. Models

2.1. Aircraft models

Three aircraft models have been used for the purpose of the evaluation of the benefits of the integrated antennas, namely NASA CRM, Fokker 100 and EV-55. Different locations of the radome along the aircraft's fuselage and several types of VHF antennas have been considered during this study.

The geometrical characteristics of all used models are depicted in Table 1.

	Chord [m]	Span [m]	Sref [m²]
CRM	7.005	58.76	383.69
F100	3.8	28.08	93.5
EV-55	1.6	16.1	25

Table 1: Geometric characteristics of used aircraft models

2.1.1. NASA Common Research Model (CRM)

The NASA CRM [1] designed by Boeing and among other purposes has been used during the Drag Prediction Workshops (DPW) [2] to obtain the experimental data for CFD code verification. It is based on a transonic transport configuration designed to fly at a cruise Mach number, $M = 0.85$ at design lift coefficient $CL = 0.5$. Several configurations of the CRM can be used. The horizontal tail and nacelle/pylon can be integrated into the baseline configuration which contains the wing and body, only. The CRM model used for this study is depicted in Figure 3. The considered baseline configuration corresponded to the wing, body, and horizontal tail, without radome. The CRM model is representative for a large twin-aisle aircraft, such as A350 or Boeing787.

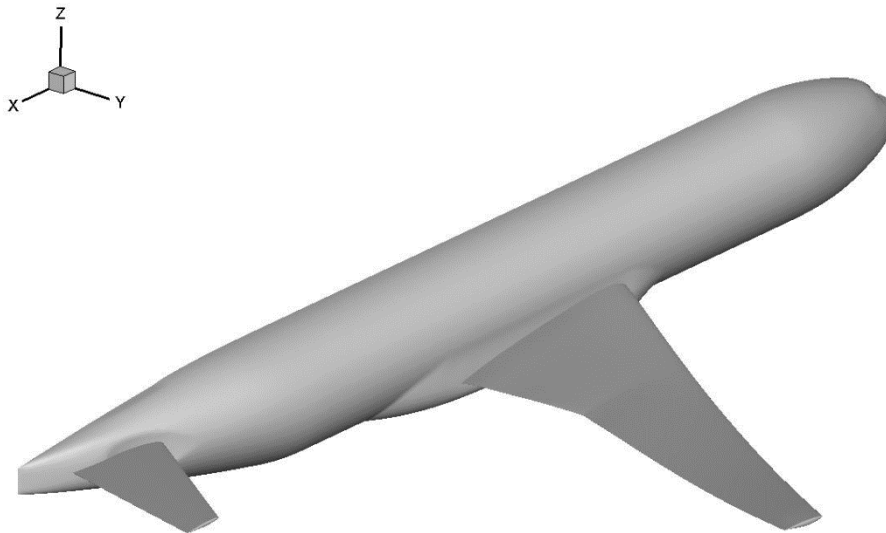


Figure 3: Baseline configuration of Common Research Model

2.1.2. Fokker 100

The Fokker 100 is a medium-sized, twin-turbofan jet airliner from Fokker. It was used to evaluate the effect of the GoGo-2Ku-like radome (see Figure 2) and VHF communication antennas on the middle size aircraft. The Computer Aided Design (CAD) model used for CFD simulations was geometrically simplified in comparison with the real aircraft, e.g. the shape of the wind screen was simpler, nacelles were flow-through type and the model did not have a dorsal fin.

2.1.3. EV-55

For the evaluation of the effect of the VHF communication antennas on the drag and fuel consumption the EV-55 Outback aircraft was used (see Figure 11). It is a twin-engine turboprop aircraft that was designed by Evекtor-Aerotechnik. Three different types of VHF antennas were considered during this study. More details are in the following sections.

2.2. Antennas

2.2.1. Radome

The radomes of Panasonic-like and Gogo-2Ku-like and were placed on the fuselage of CRM. The Gogo-2Ku-like radome was used for simulations of drag increment of Fokker 100 aircraft. The Gogo-2Ku-like radome has a lower profile than the Panasonic-like radome, because the antennas use different technologies. The GoGo-2Ku antenna consists of two large aperture phased-array antennas with advanced electronic beam forming and steering capabilities. The Panasonic antenna also contains planar phased array antennas, but the steering to satellites uses mechanical steering. The Panasonic and GoGo-2Ku antennas are shown in Figure 4 and Figure 5, respectively.

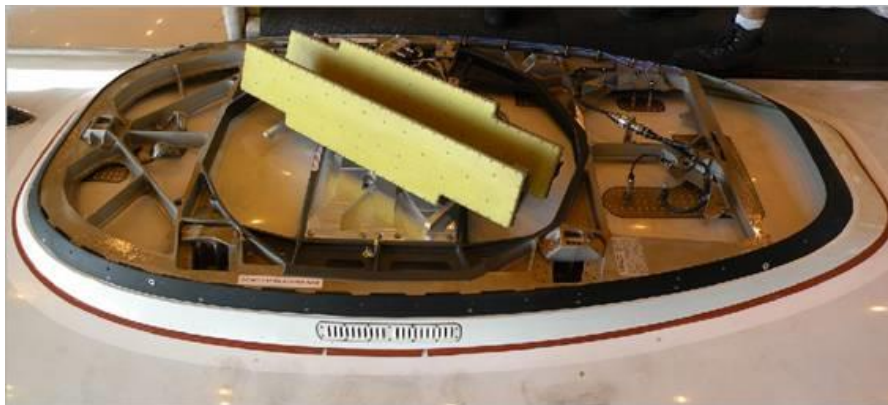


Figure 4: Panasonic Ku-band antenna



Figure 5: GoGo-2Ku antenna (left receive, right transmit)

The comparison of the shapes of the Gogo-2Ku-like radome with the Panasonic-like radome is depicted in Figure 6. Three different locations along the fuselage of CRM were considered, namely forward (marked G1 in following figures), over wing (marked G3) and rear (marked G2) positions. The Gogo-2Ku-like and Panasonic-like radomes were positioned in the same places along the fuselage.

The positions of the radome on the fuselage of Fokker 100 resulted from the results of simulations of the baseline configuration and Pressure Coefficient (C_p) distribution along the fuselage. Three locations of the radome were considered, optimal, over wing and rear. The positions of the radome on the CRM and Fokker 100 are depicted in Figure 7. Every radome's position was evaluated separately. The optimal position on Fokker 100 was determined according to the C_p distribution along the fuselage to place the radome to the area of as low as possible local velocity (see Figure 8).

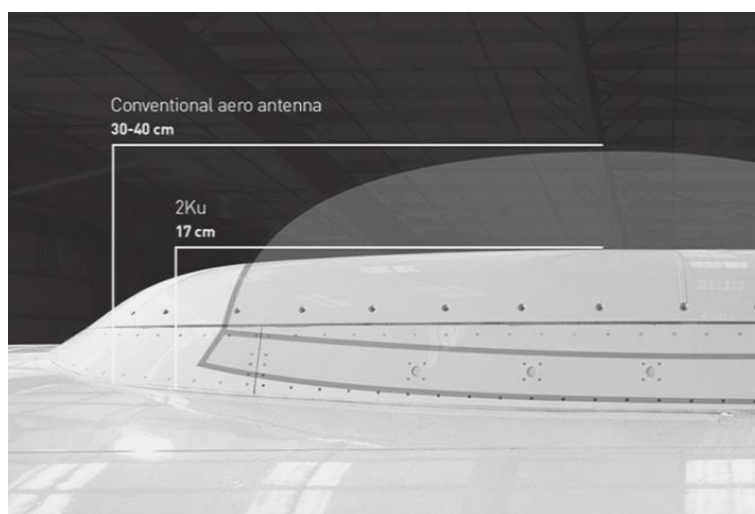


Figure 6: Comparison of Gogo 2Ku-like and conventional (Panasonic-like) radome (adopted from [3])

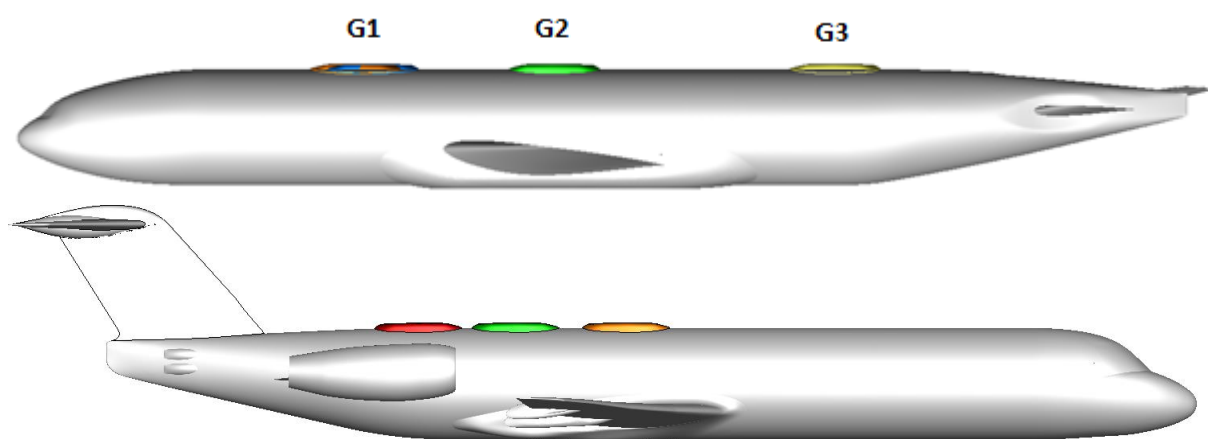


Figure 7: Positions of the radome on CRM (above) and F100 (below)

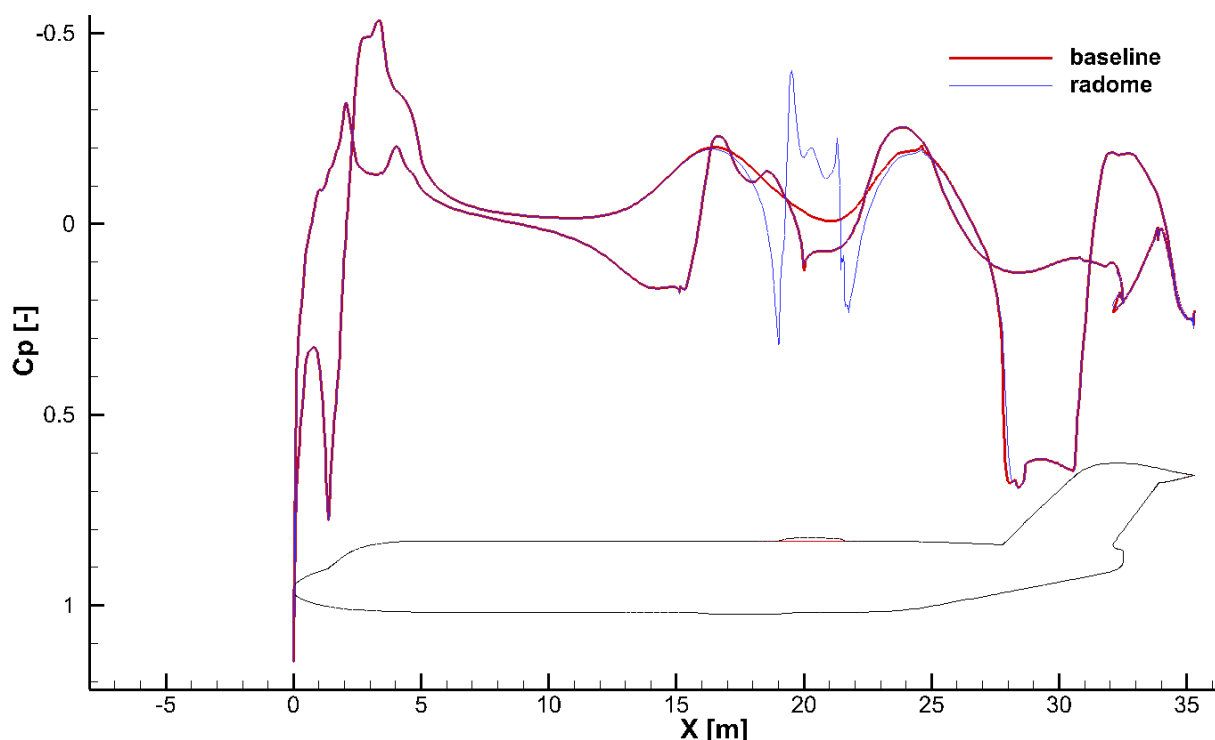


Figure 8: Cp distribution along the aircraft's fuselage

2.2.2. VHF antennas

Three types of VHF antennas (CI-108-L, CI-119 and CI-211) were placed on the fuselage of the F100 and EV-55 and their effect on drag and emissions was evaluated. The shapes of the antennas are depicted in Figure 9. The positions of the antennas are depicted in Figure 10 and Figure 11, respectively. Their locations were defined by the producers of the aircraft. The positions marked by number 12, 13 and 14 in Figure 10 were considered for F100 aircraft. Each type of antenna was evaluated separately. It means that one couple of the same type of the antenna was used during the particular simulation.

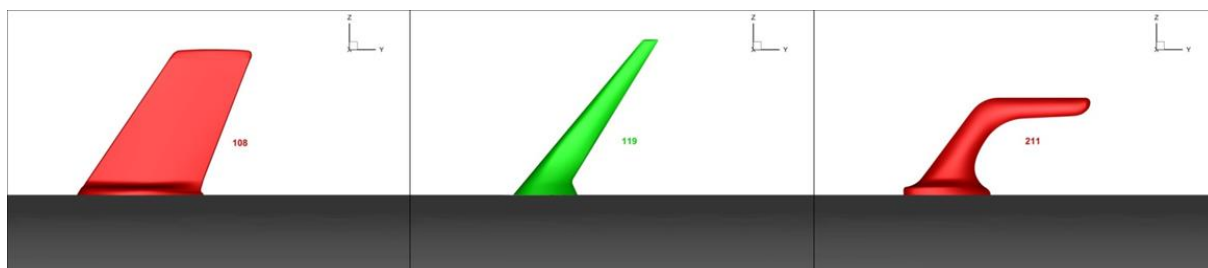


Figure 9: VHF antennas

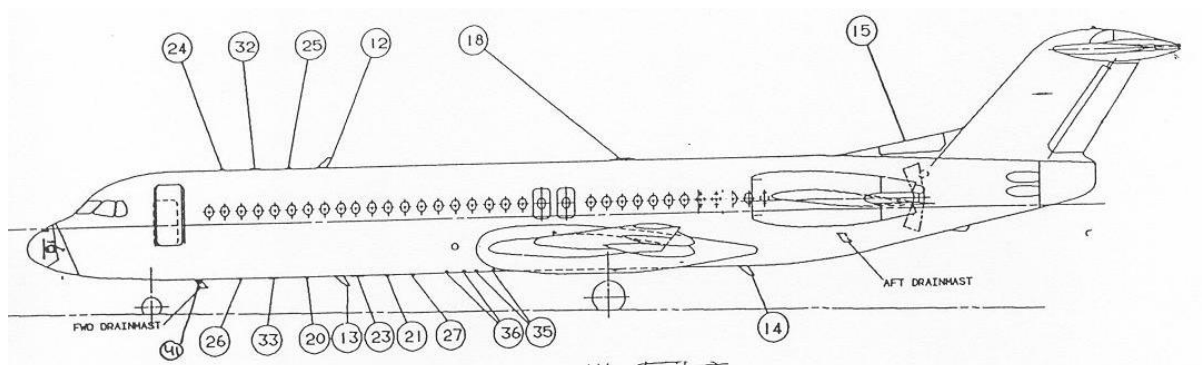


Figure 10: Positions of the VHF antennas on F100 aircraft

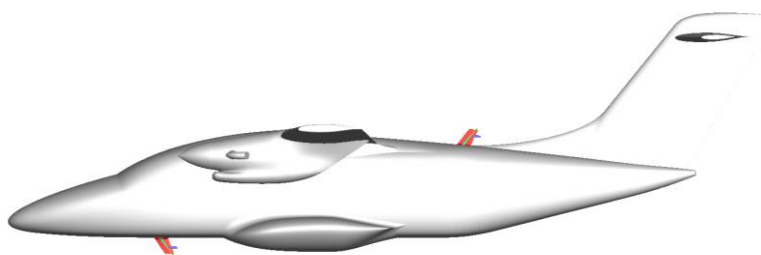


Figure 11: Positions of the VHF antennas on EV-55 aircraft

3. Methods

3.1. Grid generation and flow solver

All computational grids were generated by Pointwise software [4]. They are unstructured grids with rectangular elements on the model surfaces, prismatic layer and tetrahedron elements in the volume. The height of the first layer was set to fulfil the demand of the turbulence model on the value of the y^+ function. The grid topology was the same for all considered configurations of the radomes or VHF antennas on the particular aircraft. The differences were only in close vicinity of the radomes or VHF antennas.

The Reynolds-averaged Navier-Stokes (RANS) equations are solved using in-house CFD program. It is a finite volume Navier-Stokes solver for unstructured meshes. The $k-\omega$ Explicit Algebraic Reynolds Stress Model (EARSM) turbulence model was used for this study. All simulations were run as a fully turbulent flow. A far-field boundary condition was used on the outer boundary of the computational domain. This condition is specified by Mach number, flow direction, static pressure and static temperature. The aircraft was treated as no-slip viscous boundary. Symmetry boundary condition was used at the symmetry plane of the half model.

3.2. Flow conditions

Flow conditions used during this study are depicted in Table 2. They corresponded to the cruise regimes of particular aircraft. The angle of attack was varied during the simulations to obtain constant lift coefficients of CRM and F100 aircraft.

Aircraft	M [-]	Re [-]	C_L [-]
CRM	0.85	$30 \cdot 10^6$	0.5
F100	0.75	$22.2 \cdot 10^6$	0.45
EV-55	0.31	$11.5 \cdot 10^6$	0.18

Table 2: Flow conditions of particular simulations

3.3. Weight penalty

The weight penalty due to the presence of the radome were calculated by two approaches. The first one was introduced and used by the radome's producer [3]. It is called Aerodynamic Equivalent Drag Penalty (AEDP). It assumes that the value of the lift over drag ratio is constant during the cruise part of the flight.

$$\frac{L}{D} = C \quad (1)$$

If the drag of the aircraft is increased by the contribution of the radome, the lift has to be also increased according to the following equation.

$$L_{New} = (D + D_{Radome}) \cdot C \quad (2)$$

The differences between the new value of lift (L_{New}) and original value of lift is the AEDP.

$$AEDP = L_{New} - L \quad (3)$$

The hardware weight has to be also added to the AEDP to obtain the overall increasing of the weight by presence of the radome. The AEDP could be an equivalent to the weight of the fuel which can be saved by integrated antenna.

The second simplified method/approach is based on the Breguet equation and contribution of the fuel weight to the Maximum Take-Off Mass (MTOW) of the aircraft and the assumption of the fuel burned in cruise (see Eq. 4 and 5). The additional fuel needed to carry the radome consists of the fuel needed for radome's weight and fuel needed for radome's drag. It can be divided into the part needed for the radome's drag itself and part needed for radome's drag fuel (additional fuel needed to carry the extra fuel needed because of the radome's drag – snow ball effect). This method was applied to three aircraft, A350, B-787 and F100. The A350 and B-787 have been selected because of their geometric and also cruise regime similarity in each other and also in CRM. The F100 was used to evaluate the effect of integrated antenna on medium-sized aircraft.

$$\Delta m_{f,sys} = m_{sys} \cdot (e^{k_{br}t} - 1) \quad (4)$$

$$k_{br} = \frac{SFC \cdot F}{m} \quad (5)$$

3.4. Carbon Dioxide (CO₂) and Nitrogen Dioxide (NO_x) emissions

The combustion of hydrocarbon fuels with air in aircraft engines produces CO₂ and Dihydrogen Monoxide (H₂O), water vapour, as main combustion products. According to [7], it can be assumed that emissions of CO₂ and H₂O are proportional to fuel consumption, with constant emission indices of 3155 g/kg for CO₂ (i.e. gram emissions per kg fuel burned) and 1237 g/kg for H₂O.

Emissions of NO_x, Carbon Monoxide (CO), Hydrocarbons (HC) are influenced by a number of parameters, most prominently the engine type, its power setting, current flight speed, altitude and ambient atmospheric conditions. Respective emission indices vary significantly depending on the above parameters. While emissions of NO_x are mainly produced at high engine power settings, products of incomplete combustion like CO and HC are mostly emitted at low engine power levels. The NO_x and CO emissions in dependence on fuel consumption for an ideal engine are depicted in Figure 12.

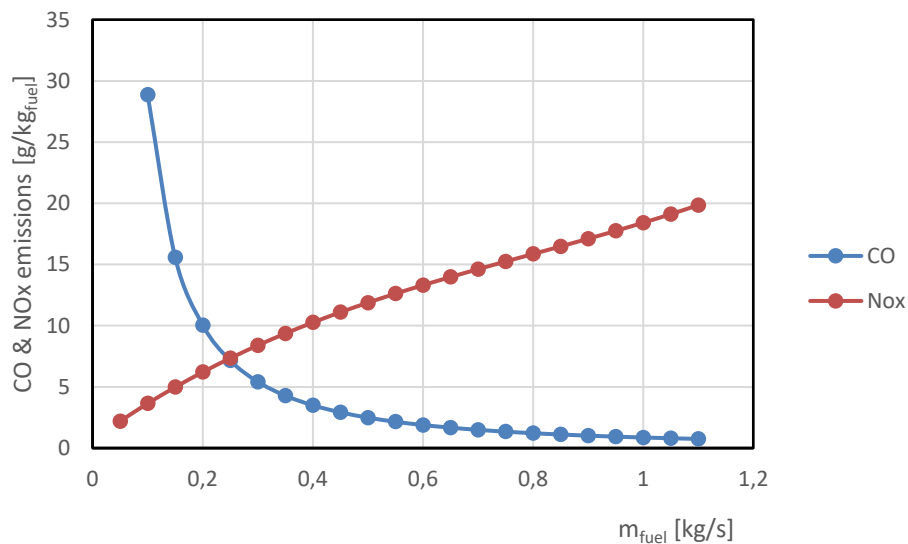


Figure 12: CO and NO_x emissions for ICAO Aircraft Engine Emissions Databank engine [6]

The NO_x emissions can be estimated by several methods. One of these methods is the calculation of the emissions from the chemical reactions inside the combustion chamber using its efficiency and selected regime [5]. Another method is based on the data provided by the engines' manufacturers. International Civil Aviation Organisation (ICAO) manages the aircraft engine emission databank database [6], where the fuel consumptions and emission of particular engines are defined. The output from this database can be partially

used in connection with the results of this study to evaluate the effect of integrated antennas with the aircraft's surface in terms of CO₂ and NO_x emission for different parts of the flight. It has to be connected with the specific aircraft and its engine to obtain relevant figures. However, the data from the database are valid only for low altitude, because of the main purpose of evaluation of the local emissions in close proximity of the airport.

Another method of calculation of the production of the emissions is based on fuel flow, speed, and altitude. The Boeing-2 fuel flow method (e.g. [7]) was used to calculate the NO_x emissions along the flight profile. Boeing-2 fuel flow method is a well-accepted, standard method of estimating NO_x. Integration along the flight profile yields NO_x emissions and fuel burn. A flight profile consists of a chain of flight segments. Generation of a flight profile starts with a first estimate of a take-off weight (based on OEW, payload, distance-based fuel estimate and reserve fuel estimate). During the flight fuel is burned, and the aircraft weight continuous adjusted accordingly. Fuel burn is based on momentary weight, speed, altitude and thrust setting. The resulting momentary (fuel) weight at touchdown is used to correct the initial calculated/estimated fuel weight until remaining fuel after landing equals reserve fuel.

The NO_x emissions have been calculated for the reference aircraft A350-900 and Fokker100 during typical flights. More details are presented in the section Results.

4. Results

4.1. Effect of the location of the radome on the drag

The effect of the radome placed in different location along the fuselages of CRM and F100 has been evaluated from the drag point of view. The drag of the aircraft with different locations of the radome was evaluated for the constant lift coefficient (see Table 2). It means that the angles of attack were slightly different for different radome locations to obtain the same CL and hence aerodynamic loading.

4.1.1. Common Research Model

The drag increment, caused by the presence of the different radomes in particular locations, is depicted in Figure 13. The drag is increased from 0.07% up to 0.75% corresponding to the Gogo-2Ku-like radome and from 0.13% up to 1.24% corresponding to the Panasonic-like radome. All increments are related to the baseline configuration. The drag of the baseline CRM and the CRM with Gogo-2Ku-like and Panasonic-like radome in different positions along the fuselage is in Figure 14 and also in Table 3. Both of the radomes' shapes have the same trend of the drag increment. The best positions of the radome are in the front and in rear part of the fuselage while the overwing position (marked as G_2 in Figure 13) is the worst. The higher drag in the overwing position is most probably due to the locally accelerated flow caused by the wing (circulation). The C_p distribution along the fuselage is depicted in Figure 15. It can be seen the locally accelerated flow just behind the nose of the fuselage and overwing position (the wing root is between the 25m and 37m in x coordinate). The suitable position for placing the radome can be determined according to the C_p distribution with lower local flow velocity, in front of the wing and in the aft part of the fuselage, respectively. It must be mentioned, that the drag of the rear position is slightly biased due to the missing the vertical tail plane.

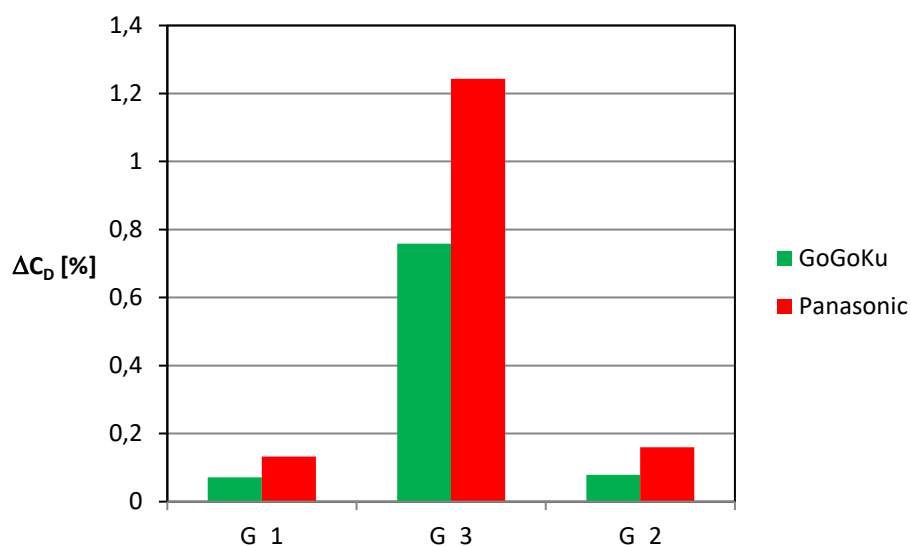


Figure 13: Drag increment of CRM by presence of the radomes in different locations

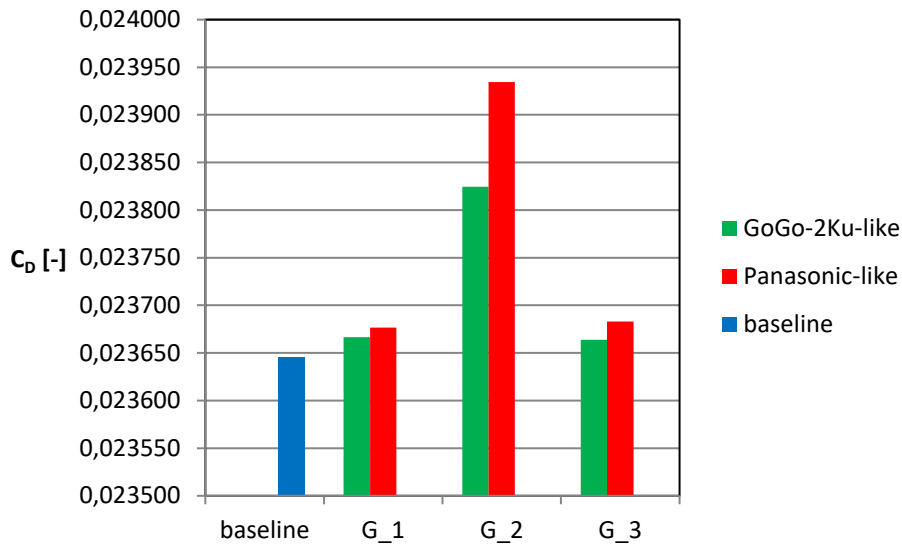


Figure 14: Drag coefficients of particular radome's configurations

	baseline	GoGo-2Ku-like			Panasonic-like		
		G_1	G_2	G_3	G_1	G_2	G_3
CD [-]	0,023645	0,02366656	0,0238245	0,0236639	0,023677	0,023935	0,023683

Table 3: Drag coefficient of the baseline and particular CRM's configurations with radomes (see Figure 7)

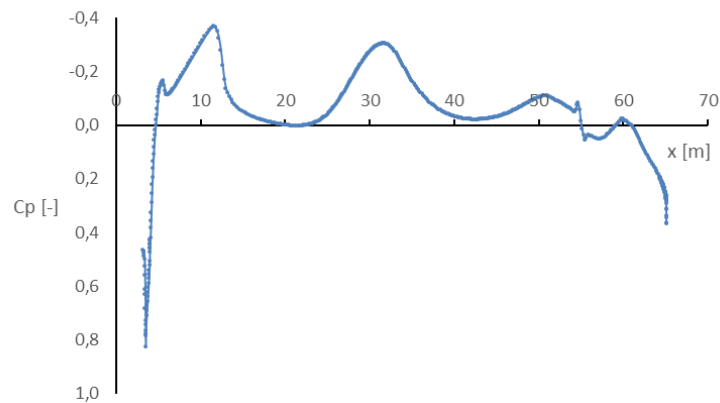


Figure 15: Cp distribution along the fuselage of the baseline configuration

4.1.2. Fokker 100

The position of the Gogo-2Ku-like radome on the F100's fuselage was determined on basis of the C_p distribution along the fuselage (see Figure 8 and Figure 16) in order to obtain the best position with the smallest drag increment. This position is depicted and marked opt in Figure 17. Two additional radome's position (over wing and rear) were evaluated for the purpose of ascertain if the determined position is the best. The drag coefficients of particular considered configurations are depicted in Figure 17. The drag increment based on the baseline configuration without radome is depicted in Figure 18. It is possible to see that the determined position is the best and the drag increment due to presence of radome

is 0.23% while the drag increment of the rear position is by about 0.34% and over wing position is by about 0.79% higher related to the baseline.

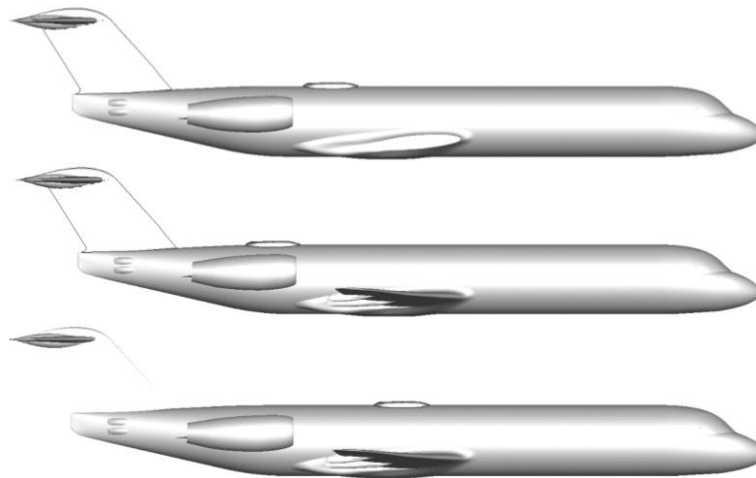


Figure 16: Radome's locations, optimal (upper), rear (middle) and over wing (bellow)

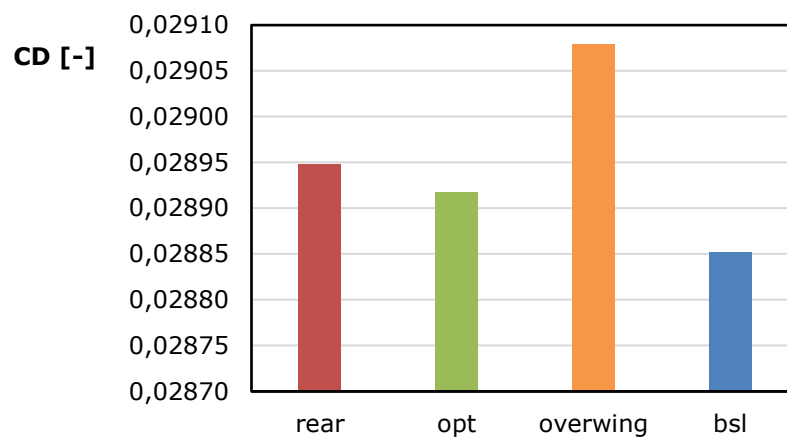


Figure 17: Drag coefficients of particular radome's configurations

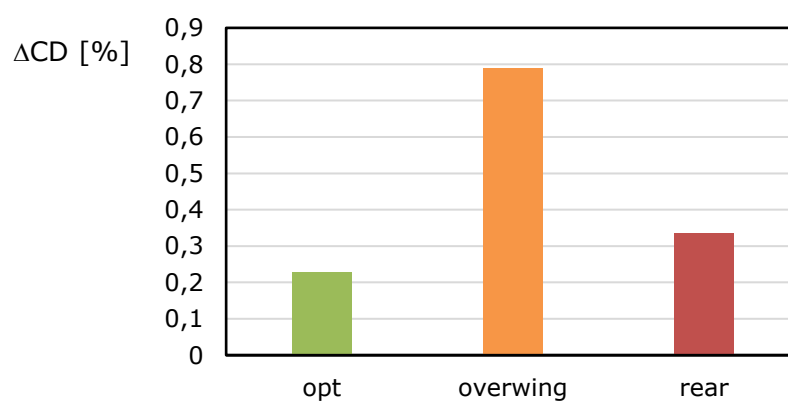


Figure 18: Drag increment due to the presence of radome

4.2. Weight penalty

The weight penalty was evaluated by means of two methods described in section 3.3, namely AEDP and weight penalty. The AEDP method was used in connection with the CRM and its characteristics. The weight penalty approach was used for two reference aircraft (A350 and B-787) and for F100, because of availability of their characteristics (geometric and weight).

4.2.1. Radome's effect

The aerodynamic characteristics of the CRM (lift, drag and radome's drag) have been used to calculate the AEDP. The values of AEDP were calculated by means of the Eq. 1-3. This method considers the aerodynamic characteristics of the aircraft only. The hardware weight of the radome was not considered during the calculation of the values of AEDP. The results of AEDP are depicted in Figure 19 (left). It can be seen that over wing position of the Gogo-2Ku-like radome is the worst with almost 1700 kg of AEDP. The others (forward and rear) positions give almost the same value of AEDP 159 kg and 178 kg, respectively. The Panasonic-like radome is slightly more penalizing than the Gogo-2Ku-like radome. The AEWP for Panasonic-like radome is from 227 kg corresponding the rear position up to 2260 kg corresponding the worst (overwing) position of the radome.

The second method of calculation of the weight penalty determines the weight of the additional fuel needed to carry the radome itself (hardware weight and radome's drag) and also some more fuel needed to carry the additional fuel weight (snow ball effect). This method takes more into account the flight profile and the ratios between MTOW, fuel weight, burned fuel during the cruise, etc. For this study two aircraft and their parameters (MTOW, fuel weight, etc.) have been used, A350 and B-787. The value of Lift/Drag (L/D) for cruise condition was considered the same for both aircraft. It could be reason for the inaccuracy in calculated weight penalty of these two aircraft (see Figure 19 right). Some other differences are caused by the geometric characteristics of the aircraft themselves (A350 is slightly larger in comparison with CRM whilst B-787 is slightly smaller [9, 10]). The results of this method are also depicted in Figure 19 (right). It could be seen that both methods gave similar results and penalize the same configuration. The columns marked by Panasonic-like correspond to the aircraft with the Panasonic-like radome. The others correspond to the Gogo-2Ku-like radome.

The results of both methods are rather informative. The precise aerodynamic, geometrical and weight characteristics of the real considered aircraft need to be considered to obtain correct absolute values of the weight penalty. On the other hand, the trend of the effect of the radome in particular positions can be used from this procedure.

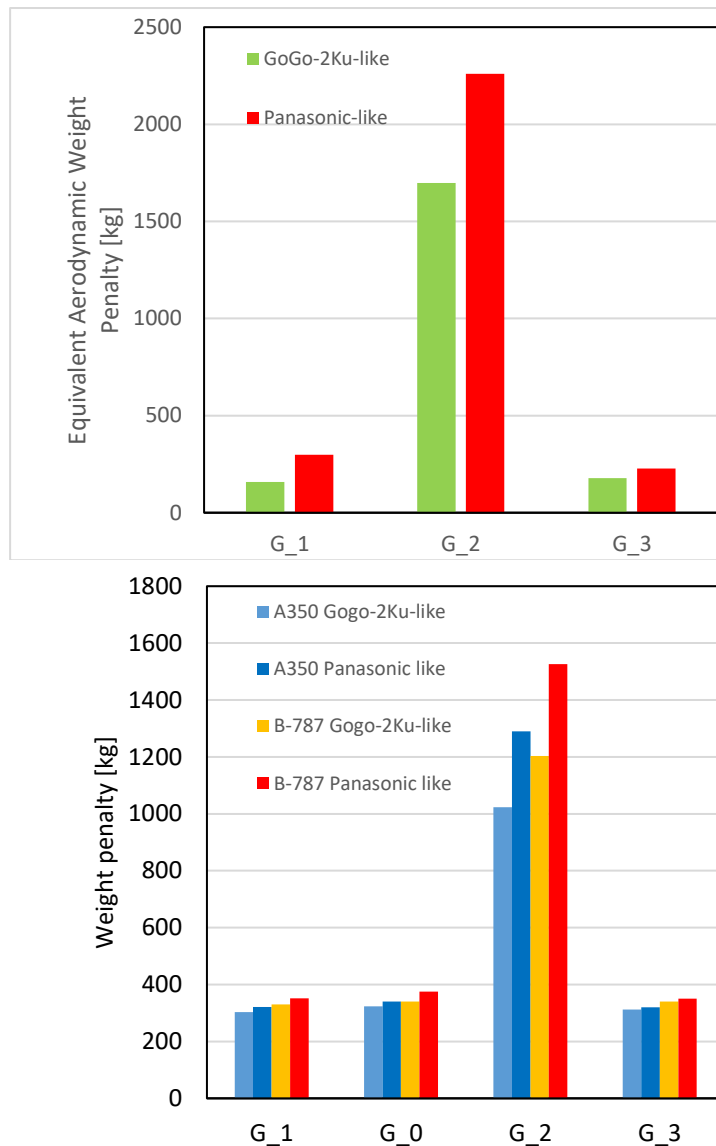


Figure 19: Aerodynamic Equivalent Drag Penalty of CRM (left) and weight penalty for two aircraft with different radome's shape (right)

The weight penalty method was also used to calculate the additional fuel need to carry the Gogo-2Ku-like radome on F100's fuselage. The aerodynamic characteristics have been used from the simulations and particular weights was taken over from the official web site [11]. The lowest weight penalty was achieved for the optimal position of the Gogo-2Ku-like radome (see Figure 20). This position was selected on the basis of the C_p distribution along the fuselage. The other two positions, over wing and rear gave little bit higher values of weight penalty by about 17 kg and 3 kg in comparison with the weight penalty of the optimal position, respectively.

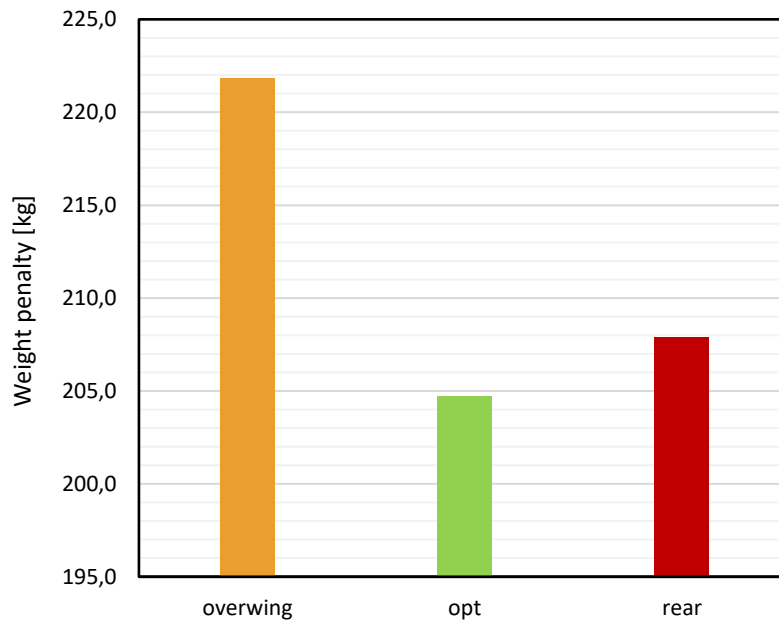


Figure 20: Weight penalty of Fokker 100

4.2.2. Effect of VHF antennas

The effect of VHF antennas on the drag and weight penalty was evaluated for the F100 and EV-55 aircraft. The same flow conditions as for the simulations of radome effect was used for the F100 aircraft. The results are depicted in Figure 21. It can be seen, that the effect of the blade antennas on the weight penalty is almost negligible. The bigger benefit of the integrated antenna is the decreasing of the probability of damaging of the protruding blade antenna by collision with the airport cars, e.g.

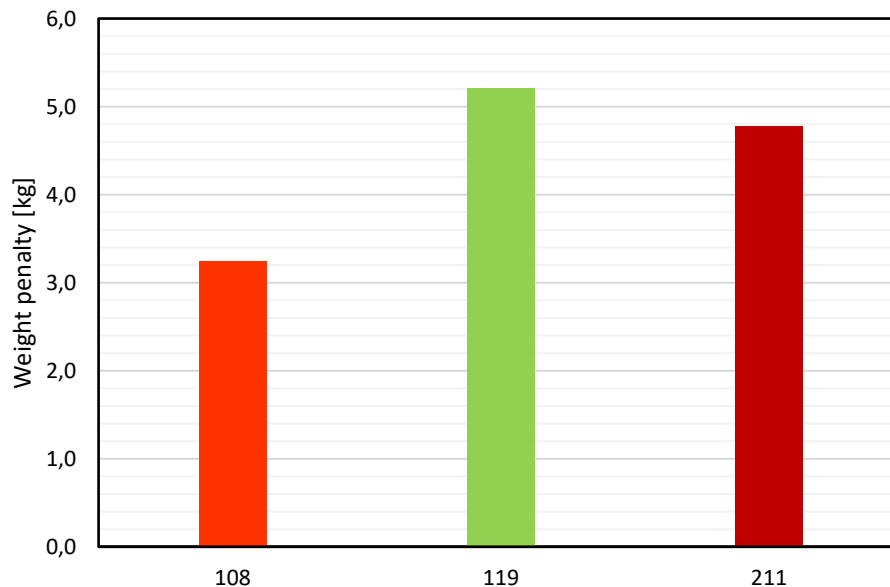


Figure 21: Weight penalty of blade antennas of Fokker 100

The similar almost negligible effect on the weight penalty has been found during simulations of the EV-55 with blade antennas (see Figure 22).

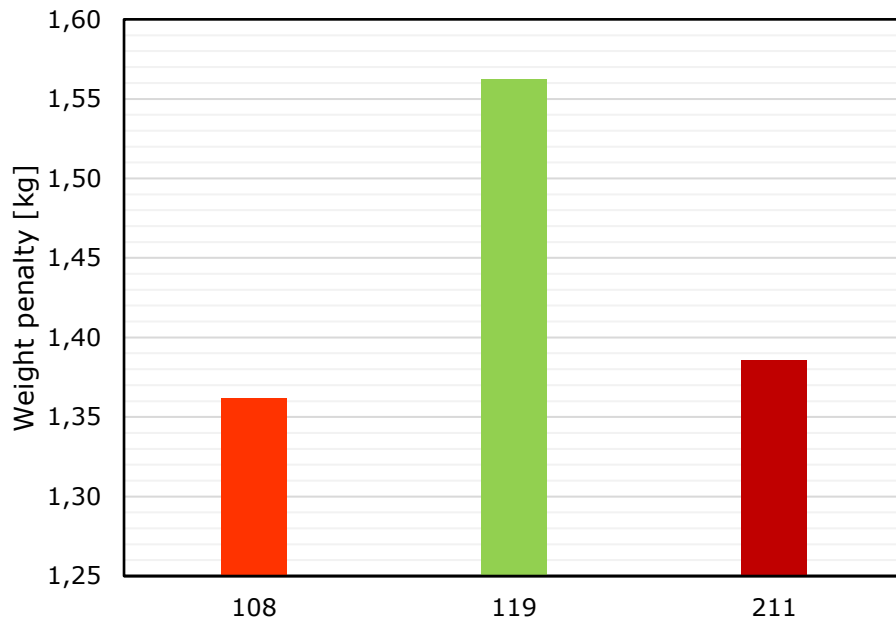


Figure 22: Weight penalty of blade antennas of EV-55

4.3. Possible reduction of the CO₂ and NO_x emissions by integrated antennas

The NO_x emissions production of the A350-900 aircraft w/o Gogo-2Ku-like and Panasonic-like radome during typical flights (7000 km and 9000 km trips, respectively), and Fokker 100 aircraft with Gogo-2Ku-like radome during typical flight (2000 km) were calculated. The values of the drag increment have been taken over from the simulations of CRM and Fokker 100 aircraft. These corresponded to the worst case (over wing location, G_2) and the rear location (G_3) and overwing and optimal location of the radomes, for CRM and Fokker 100 aircraft, respectively. The results of the estimation of the NO_x production together with the estimation of the fuel consumption are in the following tables. The values correspond to the model of A-350 with Gogo-2Ku-like radome. From Table 4 it is possible to see the savings of the amount of the fuel burned (~0.6%) and NO_x emissions produced (~2%) during the flight corresponded to the over wing radome's location (G_2) and negligible savings for the rear radome's location (G_3).

	no radome	Radome G_2	Radome G_3	
fuelburn	51760	52076	51764	[kg]
fuelestimate (incl. reserves)	53872	54388	53878	[kg]
time	531	531	531	[min]
travel distance	7004	7004	7004	[km]
takeoff mass	238154	238540	238159	[kg]
NO _x emissions	1901	1942	1901	[kg]

Table 4: Results of the estimation of the emission production for typical flight of A350-900 (7000 km) w/o Gogo-2Ku-like radome

The results of the NO_x emission production and fuel consumption corresponding to the A-350 model with Panasonic-like radome are in Table 5. It is possible to see the savings of the amount of the fuel burned (~1.22%) and NO_x emissions produced (~2.47%) during the

flight corresponded to the over wing radome's location (G_2) and negligible savings for the another radome's locations (G_3).

	no radome	Radome G_0	Radome G_2	Radome G_3	
fuelburn(integral)	77555	77654	78510	77672	[kg]
time	641	641	641	641	[min]
travel distance	9004	9004	9004	9004	[km]
takeoff mass	268358	268437	270635	268455	[kg]
NO _x emissions	1702	1706	1744	1706	[kg]
NO _x diff		3,9	42,1	4,6	[kg]
NO _x diff		0,2	2,5	0,3	[%]

Table 5: Results of the estimation of the emission production for typical flight of A350-900 (9000 km) w/o Panasonic-like radome

With reference to Table 4 and Table 5 it can be expected that the reduction of CO₂ emissions will be by about 0.6% and 1.22% for the Gogo-2Ku-like and Panasonic-like radomes, respectively, installed at the worse location G_2 are being replaced by a conformal (flush integrated) Ku-band antenna as developed in the ACASIAS project [12]. This follows from the relative difference of fuel burn between the radome at location G_2 and flush antenna (baseline – no radome configuration). When the radome is installed at position G_3 or G_0, then the savings of CO₂ are negligible.

The direct comparison of two types radome is not possible due to the different flight parameters which have been used during the calculation of the emission production. The most amount of NO_x is produced during the take-off and climb segments of the flight. The shorter the flight distance, the more dominant the climb and take-off segments are.

The typical flight parameters, like altitude, velocity, thrust, together with the fuel flow and NO_x emission depending on the time of travel are depicted in Figure 23 and Figure 24. The drag difference between two aircraft configurations is relatively small. The resulting flight profiles and NO_x emissions are then hard to distinguish in the graphs depicted in Figure 23 and Figure 24. Visually they coincide.

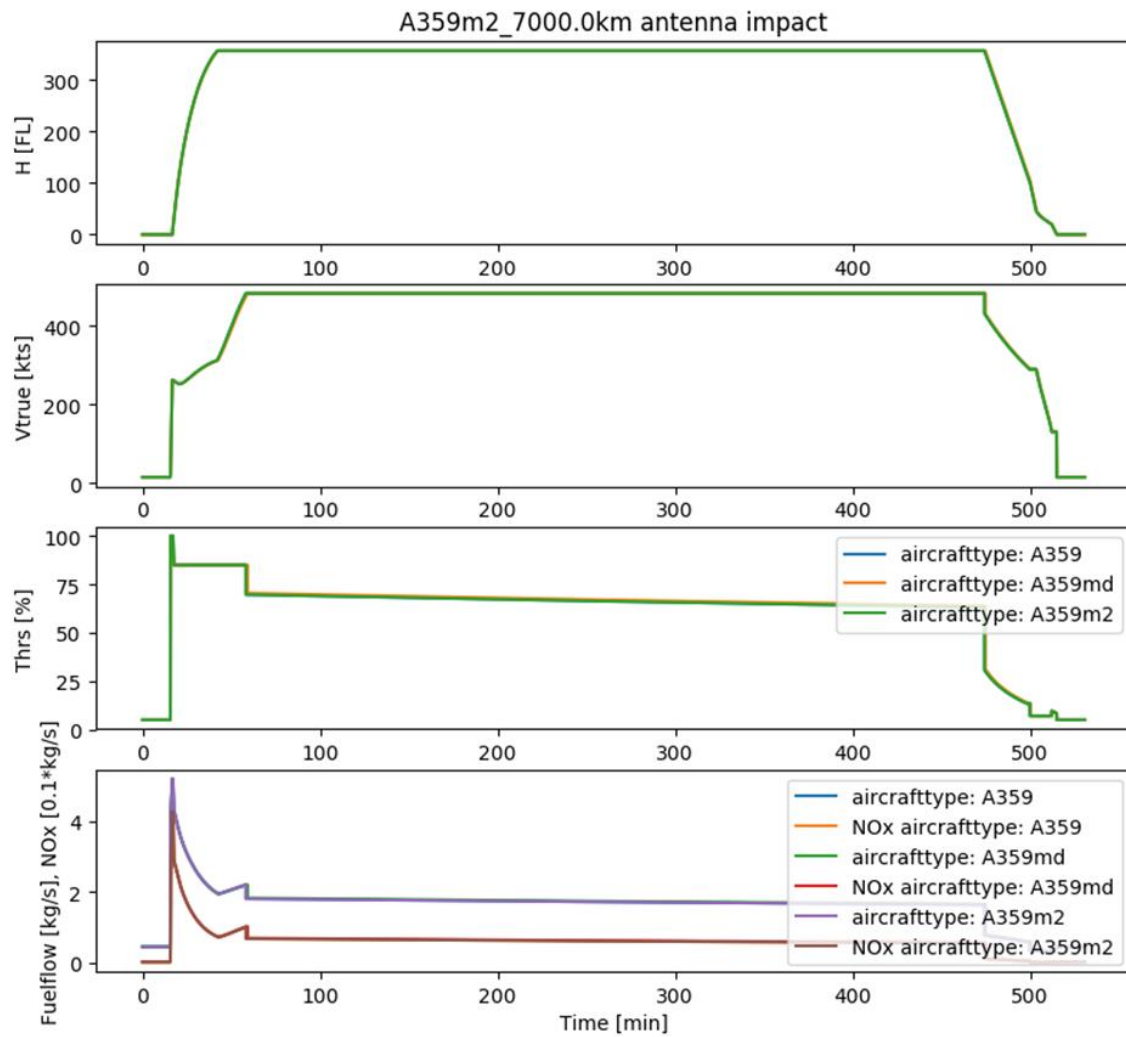


Figure 23: Fuel flow, NO_x emissions and parameters of the typical flight of A350-900 (7000 km) and Gogo-2Ku-like radome

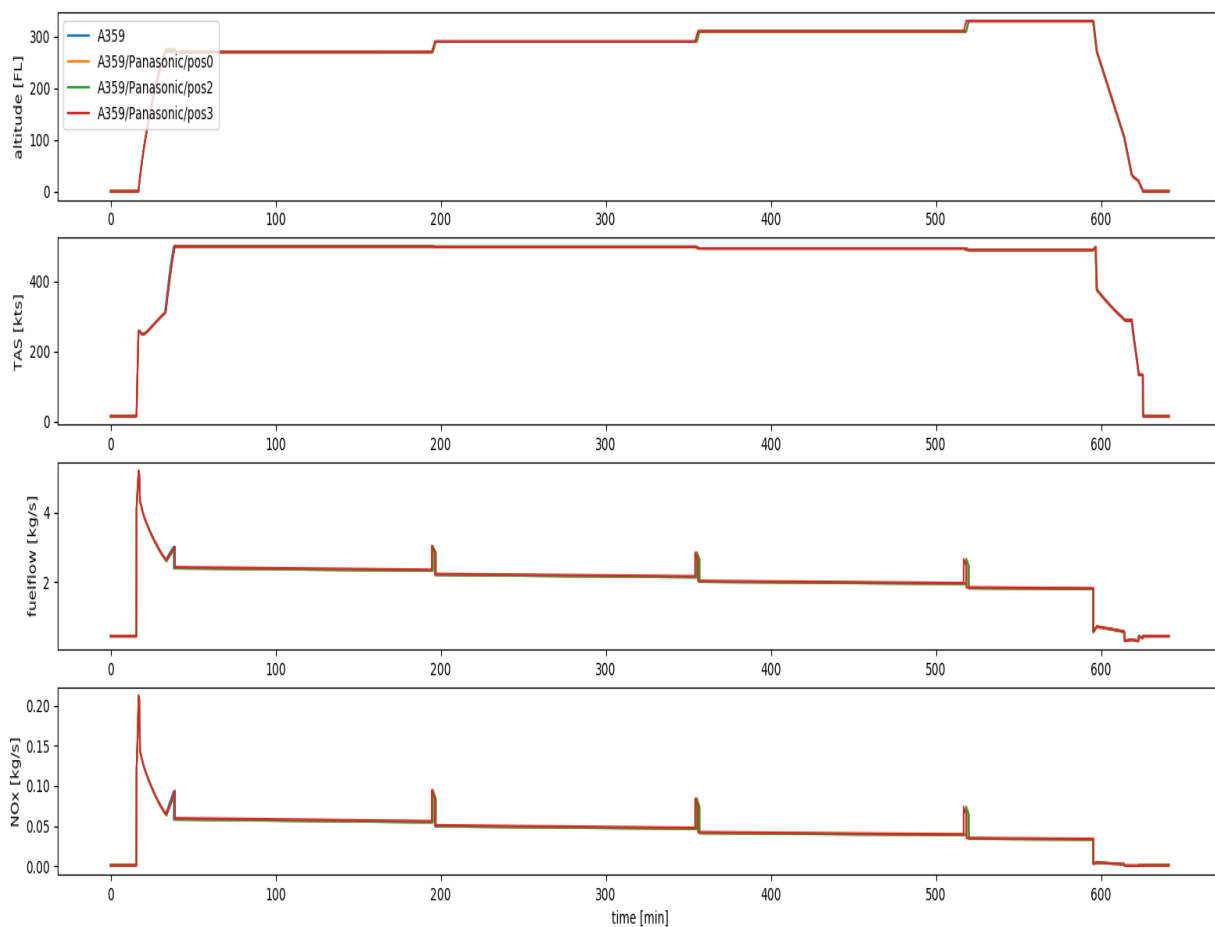


Figure 24: Fuel flow, NO_x emissions and parameters of the typical flight of A350-900 (9000 km) and Panasonic-like radome

The estimation of the NO_x emission and typical flight profile and travel distance (2000 km) of the Fokker 100 aircraft w/o GoGo-2Ku-like radome are depicted in Table 6 and Figure 25.

	no radome	optimum	overwing	rear	
fuelburn(integral)	6144	6171	6239	6184	[kg]
time	204	204	204	204	[min]
travel distance	2004	2004	2004	2004	[km]
takeoff mass	41110	41146	41231	41161	[kg]
NO _x emissions	47,6	48,0	49,1	48,2	[kg]
NO _x diff		0,43	1,47	0,64	[kg]
NO _x diff		0,9	3,1	1,3	[%]

Table 6: Results of the estimation of the emission production for typical flight of Fokker 100 aircraft (2000 km) w/o Gogo-2Ku-like radome

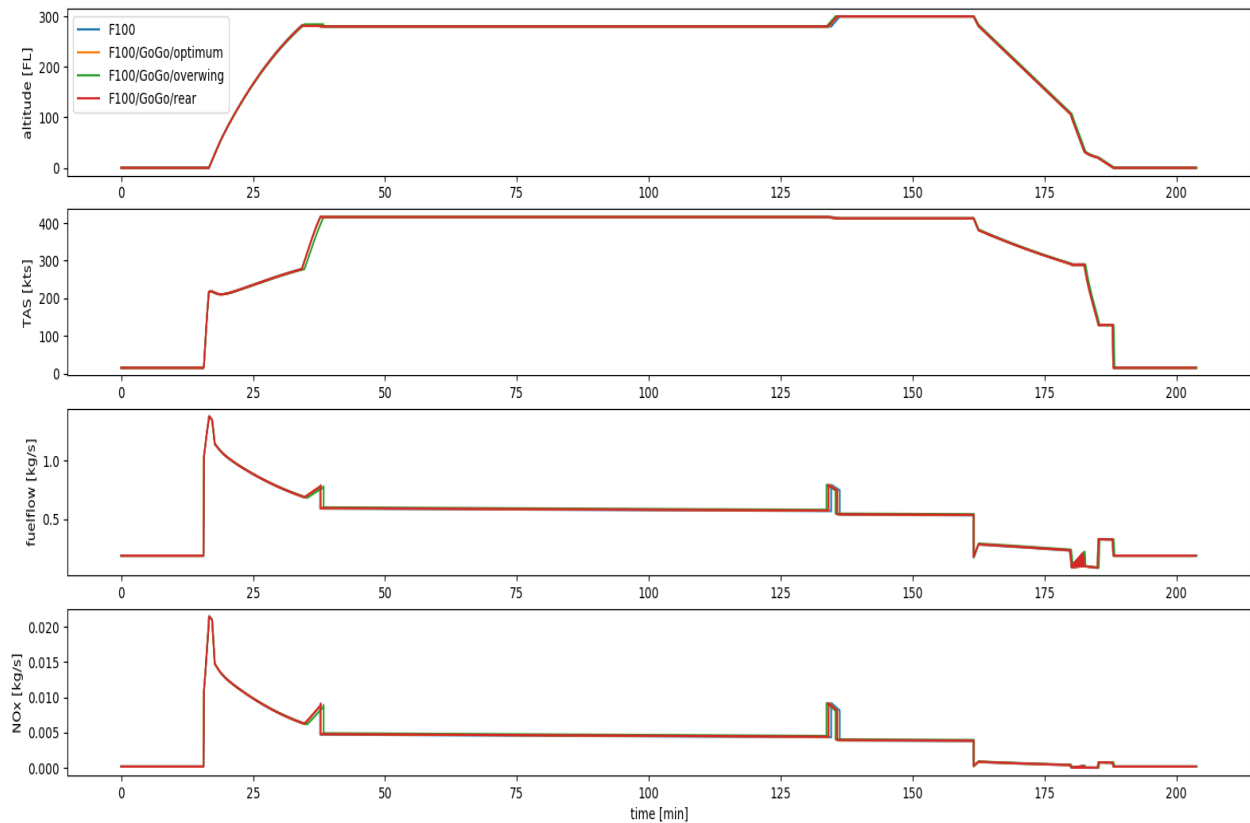


Figure 25: Fuel flow, NO_x emissions and parameters of the typical flight of Fokker 100 (2000 km) and Gogo-2Ku-like radome

With reference of Table 6 it can be expected that the reduction of CO₂ emissions will be about 0.44% and 1.52% corresponding to the optimum and overwing location of the Gogo-2Ku-like radome, respectively, by replacing the protruding antenna by the conformal (flush integrated) Ku-band antenna.

5. Conclusions

The effect of the different shapes of the radome and VHF antennas on the particular location along the fuselage of the airliner has been evaluated by CFD simulations. NASA CRM, Fokker 100 and EV-55 have been used as a reference aircraft. The values of the radomes' aerodynamic characteristics of the aircraft were used to calculate the AEDP and additional fuel which is needed to carry the radome. The method used for calculation of the additional fuel needed to carry the radome takes more into account the flight profile.

It has been found that there can be a benefit in hundreds of kilograms in case that the radome will be integrated with the aircraft's surface. On the other hand, there is almost no benefits in weight reduction of integration of the protruding VHF antennas.

From comparison of the baseline and the worst radome's configurations, it has been found that it is possible to reduce the NO_x emission of the typical flights up to 2% and 2.47% by integration of the Gogo-2Ku-like and Panasonic-like radome into the fuselage, respectively. The CO₂ emission corresponds to the fuel consumption and it can be reduced by about 0.6% and 1.22% by the integration into the fuselage of the Gogo-2Ku-like and Panasonic-like radome, respectively. There is negligible saving of the fuel consumption and emissions reduction for another location of the radome. The main benefits of this configuration are savings of the additional weight (fuel needed to carry the radome itself) and the other reasons described above.

The integrated antenna will enable to effectively utilize the length of the fuselage for placing the antenna without any negative effect on the drag cause by close proximity of the wing, e.g. The design engineer can choose the most appropriate place for the antenna from the structure, systems, and any other limitation point of views not to be limited by increasing of the drag like by using the protruding radome.

Another advantage of the integrated antenna is the reduction of the vibration, noise, maintenance costs and operational delays reducing risk to protrude parts by collisions with airport cargo cars.

6. References

- [1] Vassberg, J. C., DeHaan, M. A. Rivers, M. B. and Wahls, M. S., Development of a Common Research Model for Applied CFD Validation Studies, AIAA Paper 2008-6919. 2008.
- [2] Drag Prediction Workshop website: <http://aaac.larc.nasa.gov/tsab/cfdlarc/aiaa-dpw/Workshop5/>
- [3] GoGo website: <https://www.gogoair.com/commercial/inflight-systems/2ku/>
- [4] Pointwise website: <https://www.pointwise.com/index.html>
- [5] V. Betak, J. Kubata, Numerical prediction of soot formation in combustion chamber for small jet engines, EFM15 - Experimental Fluid Mechanics 2015, Prague, 2015
- [6] ICAO Aircraft Engine Emission Databank: <https://easa.europa.eu/document-library/icao-aircraft-engine-emissions-databank>
- [7] Schaefer, M., Bartosch, S., Overview on fuel flow correlation methods for the calculation of NO_x, CO₂ and HC emissions and their implementation into aircraft performance software, 2013
- [8] Ashok, A., Dedoussi, I. C., Yim, H. L., Balakrishnan, H., Barrett, S. R. H., Quantifying the air quality-CO₂ tradeoff potential for airports, Atmospheric Environment 99, 2014, pp. 546-555
- [9] https://en.wikipedia.org/wiki/Airbus_A350_XWB
- [10] https://en.wikipedia.org/wiki/Boeing_787_Dreamliner
- [11] https://en.wikipedia.org/wiki/Fokker_100
- [12] <http://www.acasias-project.eu/>